Chemical Engineering Journal 165 (2010) 117–121

Contents lists available at ScienceDirect

Chemical Engineering Journal

journal homepage: www.elsevier.com/locate/cej

Recyclable Fe_3O_4/hydroxyapatite composite nanoparticles for photocatalytic applications

Zheng-peng Yang[a,*], Xue-yun Gong[b], Chun-jing Zhang[a]

[a] Institute of Materials Science and Engineering, Henan Polytechnic University, No. 2001, Century Avenue, Jiaozuo, Henan 454000, China
[b] Institute of Physics and Chemistry, Henan Polytechnic University, Jiaozuo 454000, China

ARTICLE INFO

Article history:
Received 9 April 2010
Received in revised form 11 August 2010
Accepted 1 September 2010

Keywords:
Fe_3O_4/HAP nanoparticles
Diazinon
Photocatalytic degradation
Reusability

ABSTRACT

Recyclable Fe_3O_4/hydroxyapatite (HAP) composite nanoparticles have been developed as a novel photocatalyst support, based on the embedment of magnetic Fe_3O_4 particles into HAP via homogeneous precipitation method. The resultant nanoparticles were characterized by transmission electron microscope (TEM), Fourier transform infrared (FTIR) spectrometer and X-ray diffraction (XRD). These particles are almost spherical in shape and have a unique size of about 25 nm in diameter. The Fe_3O_4/HAP nanoparticles show superior catalytic activity in the process of the diazinon degradation under UV irradiation. The superparamagnetic properties of the Fe_3O_4/HAP nanoparticles provide a convenient route for separation of the catalyst from the reaction mixture by application of an external permanent magnet. The spent catalyst could be recycled without appreciable loss of catalytic activity.

1. Introduction

With the rapid development of nanostructured materials and nanotechnology, magnetic nanoparticles have received considerable attention [1,2]. Compared with the corresponding bulk material, magnetic nanoparticles possess unique property, namely superparamagnetism, in addition to their low toxicity and biocompatibility. This means that these particles are attracted to a magnetic field but retain no residual magnetism after the field is removed [3–5]. Thus, suspended superparamagnetic particles in solution can be removed from a reaction mixture using an external magnet, but they do not agglomerate after removal of the external magnetic field. The physiochemical properties of magnetic nanoparticles enable them to have a great potential for many applications in various fields, such as magnetically assisted drug delivery [6–8], magnetic separation of biomolecules [9], magnetic resonance imaging (MRI) contrast agents [10], gene manipulation and immunoassay [11], catalysis [12,13] and enzyme immobilization [14]. In addition, iron oxides were also used as natural photocatalysts to catalyze degradation of organic pollutants in environment [15–17]. However, in practical applications, these nanoparticles exhibited some drawbacks, such as poor stability and large aggregation. It has been demonstrated that iron oxide nanoparticles encapsulation provides an efficient route to prevent their aggregation in liquid and improve their chemical stability. Iron oxide nanoparticles have been successfully encapsulated within polymer [18,19], silica [20,21] and titania [22]. In the past years, HAP, a main constituent of bones and teeth, has been used widely in such fields as bone repairs, bone implant, bioactive materials and purification and separation of biological molecules due to its excellent biocompatibility, slow biodegradation, good mechanical stability and great adsorption capacity [23–26]. The accommodation of magnetic nanocrystallites into the HAP matrix has been reported by Hara and Zhang et al. and used as a high-performance heterogeneous catalyst [27–29]. Recently, HAP has been employed as a novel photocatalyst for the degradation of organic contaminants under UV irradiation [30,31]. However, to the best of our knowledge, recyclable Fe_3O_4/HAP composite nanoparticles for photocatalytic applications have not been reported.

In the present study, Fe_3O_4/HAP composite nanoparticles with reusability and photocatalytic property were synthesized by homogeneous precipitation method. The resultant magnetic HAP nanoparticles were used for the degradation of the insecticide diazinon which was selected as a model of organic pollutants. The morphology, size, structure and magnetic properties of the resulting Fe_3O_4/HAP nanoparticles were characterized by TEM, FTIR, XRD and vibrating magnetometer. The photocatalytic activity and reusability of Fe_3O_4/HAP nanoparticles under UV irradiation were also examined in detail.

2. Experimental

2.1. Materials

$FeCl_2{\cdot}4H_2O$, $FeCl_3{\cdot}6H_2O$, NH_4OH solution (25%), $(NH_4)_2HPO_4$ and $Ca(NO_3)_2{\cdot}4H_2O$ were of analytical grade and obtained from

* Corresponding author. Tel.: +86 0391 3983000.
E-mail address: zhengpengyang@yahoo.com.cn (Z.-p. Yang).

1385-8947/$ – see front matter © 2010 Elsevier B.V. All rights reserved.
doi:10.1016/j.cej.2010.09.001

Shanghai Chemical Reagent Co. Diazinon was purchased from Sigma Chem. Co. and used as received. All other chemicals were of analytical grade and used without further purification. Deionized (DI) water (resistivity of 18 MΩ cm) was obtained from a Millipore Milli-Q Water System (Millipore Inc.), and was used for rinsing and for makeup of all aqueous solutions.

2.2. Synthesis of Fe_3O_4/HAP composite nanoparticles

The preparation steps of Fe_3O_4/HAP composite nanoparticles were described as follows. 25% NH_4OH solution (10 mL) was slowly dropped into a 30 mL aqueous solution with 1.85 mmol $FeCl_2{\cdot}4H_2O$ and 3.7 mmol $FeCl_3{\cdot}6H_2O$ with vigorous mechanical stirring (1300 rpm). The reaction mixture was heated at 80 °C for 30 min, and the medium pH was maintained at 10 by the addition of aqueous ammonia solution during the reaction. The magnetic dispersion was then stirred for 1.5 h at 90 °C upon addition of a citric acid solution (0.1 M). N_2 was bubbled throughout the reaction. Subsequently, the resultant ultrafine magnetic particles were treated by magnetic separation and washed several times by DI water, and then redispersed into an aqueous suspension (50 mL). Thereafter, 100 mL aqueous solution (pH 11) with 33.7 mmol $Ca(NO_3)_2{\cdot}4H_2O$ and 20 mmol $(NH_4)_2HPO_4$ was added dropwise into the obtained magnetic suspension over 30 min with continuous stirring. The resultant milky solution was heated to 90 °C, after 2 h, the mixture was cooled to room temperature and aged overnight. The dark brown precipitate formed was filtered, washed repeatedly with DI water until neutral, and air dried under vacuum. Finally, the as-prepared sample was calcined at 400 °C for 3 h.

2.3. Characterization

The morphology and size of the resulting Fe_3O_4/HAP nanoparticles were examined on a Hitachi model H-800 TEM at an accelerating voltage of 120 kV. Infrared spectra were recorded on Nicolet 200SXV FTIR spectrometer using a KBr wafer. X-ray diffraction was performed on a Rigaku D/MAX-RC X-ray diffractometer using Cu Kα radiation. The magnetization measurements were performed at room temperature using model 155 vibrating magnetometer. The concentration of the insecticide diazinon was determined using a Shimadzu UV-1601 UV/Vis spectrophotometer at 247 nm.

2.4. Photocatalytic experiments

The photocatalytic procedure of diazinon was described as follows. Firstly, a solution containing 10 mg/L diazinon and Fe_3O_4/HAP nanoparticles was prepared and kept in the darkness for several minutes. Subsequently, the prepared suspension was irradiated with UV light under continuous stirring, the UV lamp used was a 30 W low-pressure mercury lamp (Philips, 254 nm). After illumination for some time, the suspension was sampled and filtrated through disks to remove Fe_3O_4/HAP nanoparticles before determination of diazinon concentration. According to the change in the concentration of diazinon, the photodegradation rate (X) of diazinon versus time is given by:

$$X = \frac{C_0 - C}{C_0}$$

where C_0 is the initial concentration of diazinon, and C is the concentration of diazinon at time t.

2.5. Procedure for recycling experiment

After the photocatalytic reaction, Fe_3O_4/HAP nanoparticles were assembled on the side wall of the reactor by an external permanent magnet and the reaction solution was removed. The catalyst was washed several times with DI water, and then used to start the next run under the same experimental condition.

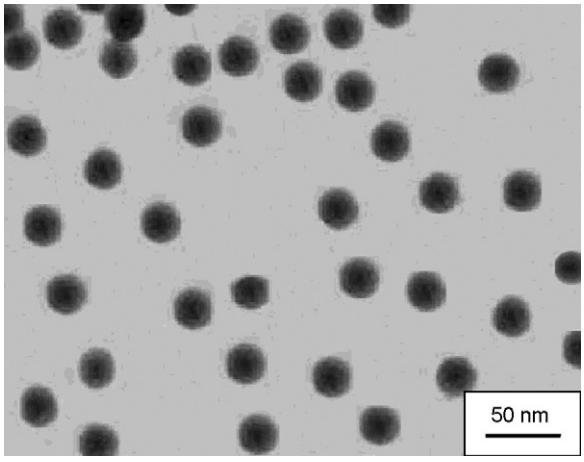

Fig. 1. TEM image of as-synthesized Fe_3O_4/HAP composite nanoparticles.

3. Results and discussion

3.1. Characterization of Fe_3O_4/HAP nanoparticles

Fig. 1 shows the morphology of the resulting Fe_3O_4/HAP nanoparticles, TEM observation indicates the as-prepared Fe_3O_4/HAP nanoparticles are almost spherical in shape, rather monodisperse and have a unique size of about 25 nm in diameter. The uniform characteristics of the Fe_3O_4/HAP nanoparticles would provide them with rapid response toward magnetic field, which is of interest to their application. Furthermore, the outer HAP shell is to avoid the corrosion of Fe_3O_4 particles and keep a stable dispersion compared to those without any protection.

Fourier transform infrared spectroscopy proved to be useful to characterize the Fe_3O_4/HAP nanoparticles. Pure HAP and Fe_3O_4/HAP nanoparticles were analyzed by FTIR (Fig. 2). It was found that all characteristic bands of HAP appeared in the IR spectrum of Fe_3O_4/HAP nanoparticles, as expected. For example, O–H stretching at 3420, O–H bending at 1650 cm^{-1}, and stretching mode of PO_4^{3-} groups at 1100, 1050 and 566 cm^{-1}. In addition, it was noted that a new band at 570 cm^{-1} appeared in the IR spectrum of Fe_3O_4/HAP nanoparticles, which was attributed to Fe_3O_4 (Fe–O

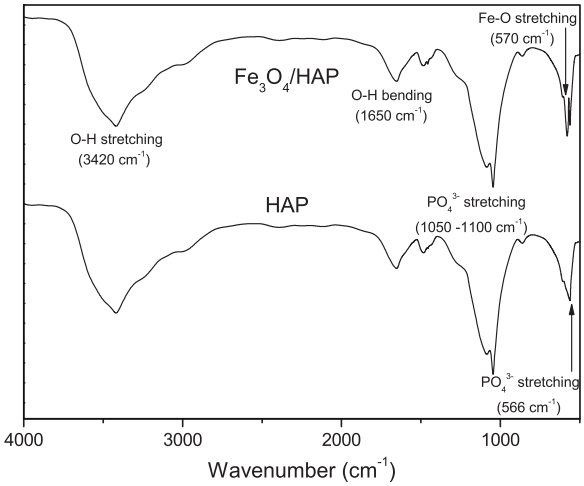

Fig. 2. FTIR spectra of HAP and Fe_3O_4/HAP composite nanoparticles.

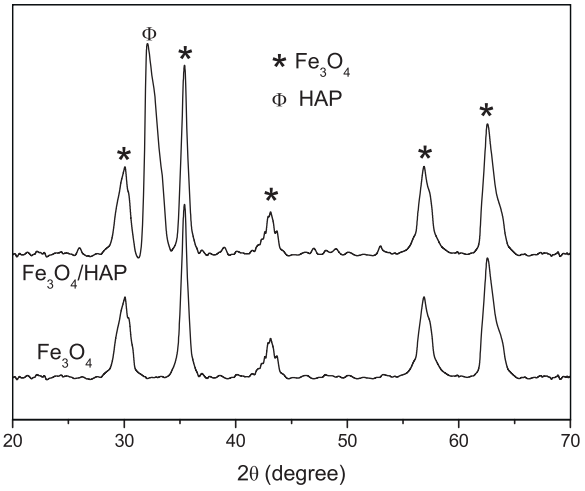

Fig. 3. XRD patterns of Fe_3O_4 and Fe_3O_4/HAP composite nanoparticles.

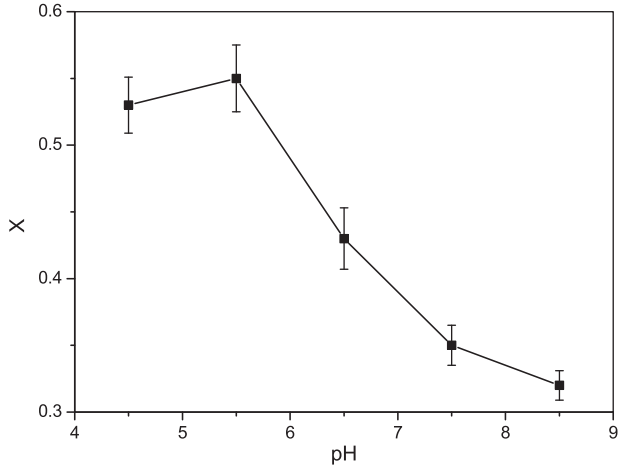

Fig. 5. Effect of pH on the photocatalytic degradation of diazinon at irradiation time of 30 min. 10 mg/L diazinon; 4.0 g/L Fe_3O_4/HAP; average of three experiments (mean ± S.D.).

stretching). Infrared analysis not only strongly confirmed the formation of Fe_3O_4/HAP nanoparticles encapsulated by HAP, but also indicated that no obvious interaction existed between Fe_3O_4 and HAP, namely Fe_3O_4 particles were embedded into HAP shell by homogeneous precipitation method. In order to further verify the presence of HAP at the surface of Fe_3O_4, XRD was employed to gain evidence for the Fe_3O_4/HAP nanoparticles. Fig. 3 shows the XRD patterns of the Fe_3O_4/HAP nanoparticles, as well as the Fe_3O_4 nanoparticles. The main peaks at $2\theta = 30.1^\circ$, 35.4°, 43.1°, 56.9°, and 62.5°, which were in agreement with the XRD peaks of pure Fe_3O_4 nanoparticles, were observed in the Fe_3O_4/HAP nanoparticles. Additionally, a comparatively broad diffraction peak at about $2\theta = 32.1^\circ$ was a characteristic peak of HAP. Thus, XRD further confirmed the formation of Fe_3O_4/HAP. Furthermore, this also revealed that the phase change of Fe_3O_4 did not take place in Fe_3O_4/HAP nanoparticles, namely Fe_3O_4 particles embedment into HAP was a physical process, which was in good agreement with the result by FTIR analysis.

The magnetic property of as-prepared Fe_3O_4/HAP nanoparticles was studied by a vibrating-sample magnetometer. As shown in Fig. 4, a weak hysteresis loop was observed, indicating that the resultant Fe_3O_4/HAP nanoparticles were superparamagnetic. From the plot of magnetization versus H, the saturation magnetization (M_s) and coercive force (H_c) were estimated to be 5.2 emu/g and 0 Oe, respectively. These magnetic properties are quite different from bulk Fe_3O_4 particles ($M_s = 84$ emu g^{-1} and $H_c = 500$–800 Oe [32]). The reduced M_s can be explained by considering the diamagnetic contribution of the HAP surrounding the Fe_3O_4 cores, which will weaken the magnetic moment, whereas the low H_c may be resulted from the size of Fe_3O_4 particles embedded into HAP. In addition, it was worth noting that the remanence of the Fe_3O_4/HAP nanoparticles was zero once the applied magnetic field was removed, which further proved the superparamagnetic behavior of the Fe_3O_4/HAP nanoparticles. Since HAP was not magnetic, the ferromagnetic properties of Fe_3O_4/HAP nanoparticles should derive from the magnetic Fe_3O_4 particles in Fe_3O_4/HAP nanoparticles. The superparamagnetic property of the Fe_3O_4/HAP nanoparticles is critical for their application in industrial catalysis, environmental protection, biomedical and bioengineering field, which prevents them from aggregation and enables them to redisperse rapidly when the magnetic field is removed.

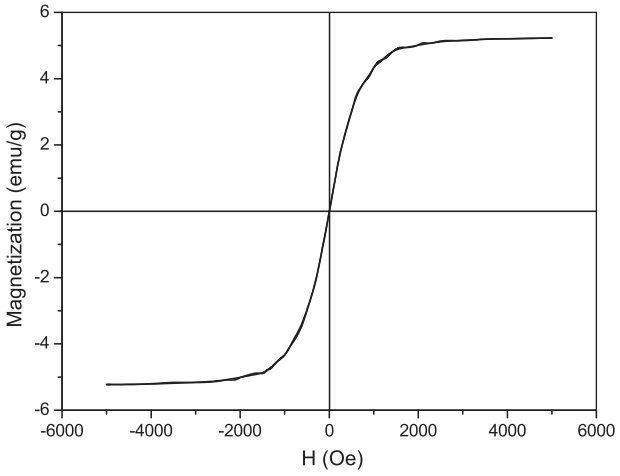

Fig. 4. Magnetization curve of as-synthesized Fe_3O_4/HAP composite nanoparticles.

3.2. Photocatalytic degradation of the insecticide diazinon in aqueous Fe_3O_4/HAP suspension

The pH values of the different wastewater are different, and it influences the photocatalytic reactions for removal of the pollutants. Similarly, the pH plays an important role in the degradation of diazinon. The effect of the initial pH from 4.5 to 8.5 on the photodegradation rate of diazinon at a fixed reaction time (30 min) is shown in Fig. 5. It was observed from the figure that the X value increased with increasing pH up to 5.5 and then decreased. Such results could be closely related to the establishment of acid–base equilibria governing the surface chemistry of nanoparticles in water. It has been reported that the ZPC (zero point of charge) of HAP is 6.8 [31], and the given pKa for diazinon is 2.6 [37]. The effect of pH on the photocatalytic performance can be thus explained in terms of electrostatic interaction between the catalyst surface and the target substrate. Such interaction would be enhanced or hindered depending on whether attractive or repulsive forces prevail, respectively. Diazinon is negatively charged at pH above 2.6, whereas HAP is positively charged at pH below 6.8. As expected, optimal interaction was found at pH 5.5, which was between 2.6 and 6.8. Thus, electrostatic attraction could be established between HAP and diazinon, exhibiting a high degradation rate.

Photocatalytic degradation of diazinon depended on the amount of the catalyst used. Fig. 6 shows the photodegradation rate of diazinon when the concentration of Fe_3O_4/HAP was varied from 2.0 to 6.0 g/L. According to Fig. 6, the X value increased with an increase

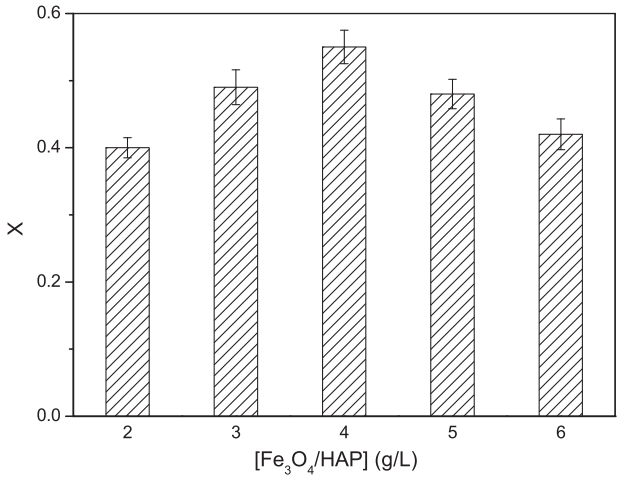

Fig. 6. Effect of Fe_3O_4/HAP amount on the photocatalytic degradation of diazinon at irradiation time of 30 min. 10 mg/L diazinon (pH 5.5); average of three experiments (mean ± S.D.).

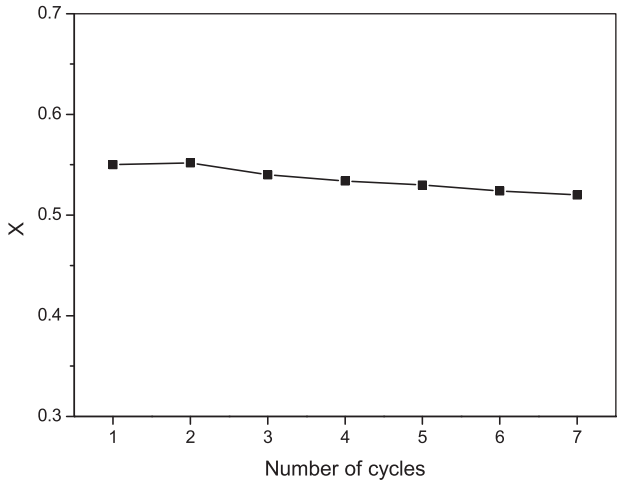

Fig. 8. Reusability of Fe_3O_4/HAP nanoparticles. Experimental condition: 10 mg/L diazinon (pH 5.5); 4.0 g/L Fe_3O_4/HAP, irradiation time of 30 min.

in Fe_3O_4/HAP concentration up to 4.0 g/L, and after that a further increase in catalyst concentration lead to a slow decrease in the *X* value. The observation can be understood from two aspects. On one hand, the increase of Fe_3O_4/HAP concentration will increase the number of photons absorbed and also the number of the diazinon molecules absorbed. And a further increase of the catalyst concentration beyond 4.0 g/L may cause light scattering and screening effects, which will hinder the penetration of light and reduce the specific activity of the catalyst. On the other hand, at high catalyst concentration, it is difficult to maintain the homogeneous suspension due to particle agglomeration, which may also reduce the catalytic activity. So the *X* value of diazinon decreases gradually. In the present study, the optimum concentration of Fe_3O_4/HAP is found to be 4.0 g/L for the degradation of diazinon.

Photocatalytic activity of Fe_3O_4/HAP nanoparticles was evaluated by monitoring the degradation rate (*X*) of diazinon selected as the deputy of organic pollutant in aqueous Fe_3O_4/HAP suspension. Fig. 7 shows the change in *X* value as a function of time during the degradation of diazinon. No obvious change in *X* value was observed in the dark, indicating that it was difficult for the degradation of diazinon in the absence of light. However, The *X* value was higher in the presence of Fe_3O_4/HAP nanoparticles and it was found that 75% removal of diazinon could be achieved in a short irradiation time, about 60 min. This was in high contrast with the 5% degradation obtained in the direct photolysis. The results demonstrated that a photocatalyst, such as Fe_3O_4/HAP was needed for the effective destruction of diazinon. Namely, the observed high degradation in the UV+ Fe_3O_4/HAP process is exclusively attributed to the photocatalytic reaction of the Fe_3O_4/HAP nanoparticles. The degradation process can be explained as follows. The band gap values of Fe_3O_4 and HAP are 5.5 eV [33] and 3.9 eV [34] respectively, HAP with low band gap is a suitable candidate to be used as a photocatalyst. In addition, the Fe_3O_4/HAP composite nanoparticles are prepared based on the embedment of magnetic Fe_3O_4 particles into HAP via homogeneous precipitation method, the outer component is mainly HAP. Thus, the photocatalytic behavior mostly lies on the HAP. When HAP is illuminated with UV light, the photo-induced electronic excitation will happen, the electronic state of the surface PO_4^{3-} group will change and create a vacancy on HAP and the electron is transferred to the surrounding oxygen followed by the formation of $^{\bullet}O_2^-$ radicals [30,35,36]. The generated superoxide radical is a powerful oxidizing agent, which can not only oxidize the diazinon molecules, but also react with water molecules and $^-$OH ions and produce $^{\bullet}$OH radicals which will further oxidize the diazinon molecules present at or near the surface of HAP.

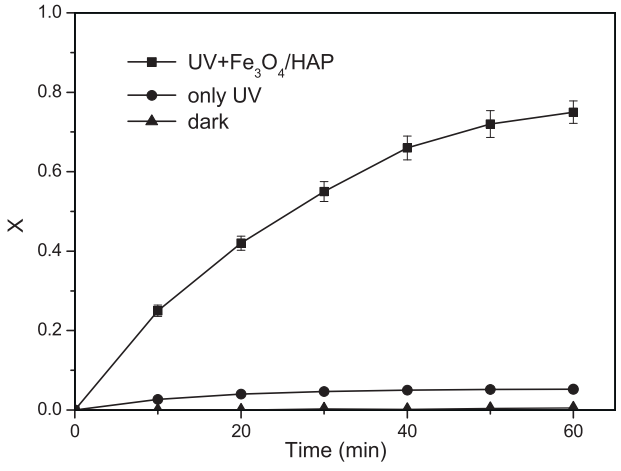

Fig. 7. The degradation of diazinon as a function of time. 10 mg/L diazinon (pH 5.5); 4.0 g/L Fe_3O_4/HAP; average of three experiments (mean ± S.D.).

3.3. Reusability of Fe_3O_4/HAP nanoparticles

Reusability of Fe_3O_4/HAP nanoparticles was evaluated by measuring the photodegradation rate of diazinon seven times under the same experimental condition and the obtained results were showed in Fig. 8. The photodegradation rate of diazinon exhibited a slight change, and kept almost 95% of the initial degradation rate till the seventh cycle. Such results demonstrate that Fe_3O_4/HAP nanoparticles can be recoverable by using an external permanent magnet and reusable with meager loss in activity during the oxidation of diazinon.

4. Conclusions

Fe_3O_4/HAP composite nanoparticles with reusability and photocatalytic property have been synthesized by homogeneous precipitation method. The analyses of TEM, FTIR and XRD reveal that the obtained nanoparticle size is about 25 nm, and Fe_3O_4 particles embedment into HAP is a physical process. The degradation experiments of pollutant indicate that Fe_3O_4/HAP nanoparticles can be employed for effective degradation of the insecticide diazinon under UV irradiation, and the optimal degradation conditions obtained are pH 5.5 and Fe_3O_4/HAP amount 4.0 g/L. Magnetic

measurement shows that Fe_3O_4/HAP nanoparticles are superparamagnetic with a saturation magnetization of 5.2 emu/g and a coercive force of 0 Oe. The superparamagnetic property of Fe_3O_4/HAP nanoparticles will prevent them from aggregation and enable them to redisperse rapidly when the external magnetic field is removed. Furthermore, recyclable measurements prove that Fe_3O_4/HAP nanoparticles can be reused without loss of high catalytic activity. The recyclable Fe_3O_4/HAP photocatalyst, we believe, will find much potential for a large variety of applications.

Acknowledgement

The authors thank financial support from doctoral foundation (reference B2009-78), Henan Polytechnic University, China.

References

[1] J.L. West, N.J. Halas, Applications of nanotechnology to biotechnology, Curr. Opin. Biotechnol. 11 (2000) 215–217.
[2] A. Curtis, C. Wilkinson, Nantotechniques and approaches in biotechnology, Trends Biotechnol. 19 (2001) 97–101.
[3] S. Stavroyiannis, I. Panagiotopoulos, D. Niarchos, J.A. Christodoulides, Y. Zhang, G.C. Hadjipanayis, CoPt/Ag nanocomposites for high density recording media, Appl. Phys. Lett. 73 (1998) 3453–3455.
[4] H.H. Yang, S.Q. Zhang, X.L. Chen, Z.X. Zhuang, J.G. Xu, X.R. Wang, Magnetite-containing spherical silica nanoparticles for biocatalysis and bioseparations, Anal. Chem. 76 (2004) 1316–1321.
[5] S.C. Tsang, C.H. Yu, X. Gao, K. Tam, Metal nanoparticle encapsulated in oxide, J. Phys. Chem. B 110 (2006) 16914–16922.
[6] G.V. Patil, Biopolymer albumin for diagnosis and in drug delivery, Drug Dev. Res. 58 (2003) 219–247.
[7] J.A. Melero, R.V. Grieken, G. Morales, Advances in the synthesis and catalytic applications of organosulfonic functionalized mesostructured materials, Chem. Rev. 106 (2006) 3790–3812.
[8] D. Astruc, F. Lu, J.R. Aranzaes, Nanoparticles as recyclable catalysts: the frontier between homogeneous and heterogeneous catalysis, Angew. Chem. Int. Ed. 44 (2005) 7852–7872.
[9] S. Mornet, S. Vasseur, F. Grasset, E. Duguet, Magnetic nanoparticle design for medical diagnosis and therapy, J. Mater. Chem. 14 (2004) 2161–2175.
[10] C. Billotey, C. Wilhelm, M. Devaud, J.C. Bacri, J. Bittoun, F. Gazeau, Cell internalization of anionic maghemite nanoparticles: quantitative effect on magnetic resonance imaging, Magn. Reson. Med. 49 (2003) 646–654.
[11] H. Nakayama, A. Arakaki, K. Maruyama, H. Takeyama, Single-nucleotide polymorphism analysis using fluorescence resonance energy transfer betwe, Biotechnol. Bioeng. 84 (2003) 96–102.
[12] X. Gao, K.M.K. Yu, K.Y. Tam, S.C. Tsang, Colloidal stable silica encapsulated nanomagnetic composite as a novel bio-catalyst carrier, Chem. Commun. 24 (2003) 2998–2999.
[13] S.C. Tsang, V. Caps, I. Paraskevas, D. Chadwick, D. Thompsett, Magnetically separable, carbon-supported nanocatalysts for the manufacture of fine chemicals, Angew. Chem. Int. Ed. 43 (2004) 5645–5649.
[14] Z.P. Yang, S.H. Si, C.J. Zhang, Magnetic single-enzyme nanoparticles with high activity and stability, Biophys. Res. Commun. 367 (2008) 169–175.
[15] J.K. Leland, A.J. Bard, Photochemistry of colloidal semiconducting iron oxide polymorphs, J. Phys. Chem. 91 (1987) 5076–5083.
[16] F.B. Li, X.Z. Li, C.S. Liu, T.X. Liu, Effect of alumina on photocatalytic activity of iron oxides for bisphenol A degradation, J. Hazard. Mater. 149 (2007) 199–207.
[17] Y. Wang, C.S. Liu, F.B. Li, C.P. Liu, J.B. Liang, Photodegradation of polycyclic aromatic hydrocarbon pyrene by iron oxide in solid phase, J. Hazard. Mater. 162 (2009) 716–723.
[18] S.P. Liu, X.H. Wei, M.Q. Chu, J.L. Peng, Y.H. Xu, Synthesis and characterization of iron oxide/polymer composite nanoparticles with pendent functional groups, Colloids Surf. B: Biointerface 51 (2006) 101–106.
[19] S. Shin, H. Yoon, J. Jang, Polymer-encapsulated iron oxide nanoparticles as highly efficient Fenton catalysts, Catal. Commun. 10 (2008) 178–182.
[20] S. Watson, D. Beydoun, R. Amal, Synthesis of a novel magnetic photocatalyst by direct deposition of nanosized TiO_2 crystals onto a magnetic core, J. Photochem. Photobiol. A: Chem. 148 (2002) 303–313.
[21] Z.L. Lei, Y.L. Li, X.Y. Wei, A facile two-step modifying process for preparation of poly(SStNa)-grafted Fe_3O_4/SiO_2 particles, J. Solid State Chem. 181 (2008) 480–486.
[22] Q.H. He, Z.X. Zhang, J.W. Xiong, Y.Y. Xiong, H. Xiao, A novel biomaterial—Fe_3O_4:TiO_2 core–shell nanoparticle with magnetic performance and high visible light photocatalytic activity, Opt. Mater. 31 (2008) 380–384.
[23] C.X. Wang, M. Wang, X. Zhou, Nucleation and growth of apatite on chemically treated titanium alloy: an electrochemical impedance spectroscopy study, Biomaterials 24 (2003) 3069–3077.
[24] T. Kokubo, H.M. Kim, M. Kawashita, Novel bioactive materials with different mechanical properties, Biomaterials 24 (2003) 2161–2175.
[25] K. Ozeki, J.M. Janurudin, H. Aoki, Y. Fukui, Photocatalytic hydroxyapatite/titanium dioxide multilayer thin film deposited onto glass using an rf magnetron sputtering technique, Appl. Surf. Sci. 253 (2007) 3397–3401.
[26] Z.P. Yang, C.J. Zhang, Photocatalytic degradation of bilirubin on hydroxyapatite-modified nanocrystalline titania coatings, Catal. Commun. 10 (2008) 351–354.
[27] T. Hara, T. Kaneta, K. Mori, T. Mitsudome, T. Mizugaki, K. Ebitani, K. Kaneda, Magnetically recoverable heterogeneous catalyst: palladium nanocluster supported on hydroxyapatite-encapsulated γ-Fe_2O_3 nanocrystallites for highly efficient dehalogenation with molecular hydrogen, Green Chem. 9 (2007) 1246–1251.
[28] K. Mori, S. Kanai, T. Hara, T. Mizugaki, K. Ebitani, K. Jitsukawa, K. Kaneda, Development of ruthenium hydroxyapatite encapsulated superparamagnetic γ-Fe_2O_3 nanocrystallites as an efficient oxidation catalyst by molecular oxygen, Chem. Mater. 19 (2007) 1249–1256.
[29] Y. Zhang, Z. Li, W. Sun, C.G. Xia, A magnetically recyclable heterogeneous catalyst: cobalt nano-oxide supported on hydroxyapatite-encapsulated γ-Fe_2O_3 nanocrystallites for highly efficient olefin oxidation with H_2O_2, Catal. Commun. 10 (2008) 237–242.
[30] H. Nishikawa, Surface changes and radical formation on hydroxyapatite by UV irradiation for inducing photocatalytic activation, J. Mol. Catal. A: Chem. 206 (2003) 331–338.
[31] M.P. Reddy, A. Venugopal, M. Subrahmanyam, Hydroxyapatite photocatalytic degradation of calmagite (an azo dye) in aqueous suspension, Appl. Catal. B: Environ. 69 (2007) 164–170.
[32] D.J. Craik, Magnetic Oxides, Part 2, Wiley, New York, 1981, p. 703.
[33] F. El-Diasty, H.M. El-Sayed, F.I. El-Hosiny, M.I.M. Ismail, Complex susceptibility analysis of magneto-fluids: optical band gap and surface studies on the nanomagnetite-based particles, Curr. Opin. Solid State Mater. Sci. 13 (2009) 28–34.
[34] D. Aronov, A. Karlov, G. Rosenman, Hydroxyapatite nanoceramics: basic physical properties and biointerface modification, J. Eur. Ceram. Soc. 27 (2007) 4181–4186.
[35] H. Nishikawa, K. Omamiuda, Photocatalytic activity of hydroxyapatite for methyl mercaptane, J. Mol. Catal. A: Chem. 179 (2002) 193–200.
[36] H. Nishikawa, Thermal behavior of hydroxyapatite in structural and spectrophotometric characteristics, Mater. Lett. 50 (2001) 364–370.
[37] N. Daneshvar, S. Aber, M.S.S. Dorraji, A.R. Khataee, M.H. Rasoulifard, Photocatalytic degradation of the insecticide diazinon in the presence of prepared nanocrystalline ZnO powders under irradiation of UV-C light, Sep. Purif. Technol. 58 (2007) 91–98.